PCCP

Accepted Manuscript

ROYAL SOCIETY OF CHEMISTRY

www.rsc.org/pccp

Cite this: DOI: 10.1039/c0xx00000x

www.rsc.org/xxxxxx

ARTICLE TYPE

On the Photophysics of 9-Amino-10-cyanoanthracene: Probing its Dual Absorption and Emission Behavior

Sharmistha Dutta Choudhury,*[a] Sukumaran Muralidharan *[,b] and Haridas Pal[a]

Received (in XXX, XXX) Xth XXXXXXXXX 20XX, Accepted Xth XXXXXXXXX 20XX

DOI: 10.1039/b000000x

The photophysics of a donor-acceptor substituted chromophore, 9-amino-10-cyanoanthracene (ACAN), has been investigated in polar and nonpolar solvents to understand its intriguing dual absorption and emission behavior. Steady-state and time-resolved fluorescence studies clearly indicate that the short wavelength emission band of ACAN arises from the higher excited singlet state, S_2, while the longer wavelength emission band arises from the intramolecular charge transfer (ICT) state, S_1. Interestingly, both these states can be populated by direct excitation from the ground state. Temperature dependent studies reveal a pronounced activation controlled nonradiative decay channel for the ICT state of ACAN. It is proposed that this activation controlled nonradiative de-excitation arises because of a large relative displacement and a cross-over of the potential energy (PE) surfaces of ACAN in the ground and the ICT states, as a result of different twist angles of the amino group in these two states. Qualitative PE diagrams have accordingly been presented to correlate and rationalize the observed results. Present study also brings to light the interesting excited state prototropic behavior of ACAN and the consequent modulation in the ICT emission that is not reported in the literature so far.

Introduction

Organic chromophores substituted with electron donor and acceptor groups that show intramolecular charge transfer (ICT) characteristics are widely investigated because of their fascinating photophysical properties[1-7] and extensive applications in diverse areas.[8-17] These molecules are suitable as metal-ion sensors, laser dyes, probes for biological structures, reporters of polarity, viscosity or temperature of microenvironments and also for development of materials with nonlinear optical (NLO) properties. Understanding the mechanism behind the interesting photophysics and optical response of such molecules is essential for effective utilization of their vast application potential.

Among many donor-acceptor substituted chromophores, the most widely studied, and one that still continues to attract research attention, is 4-(dimethylamino) benzonitrile (DMABN).[18,19] This molecule shows dual emission bands; the blue emission arising from the locally excited (LE) state and the red emission from the ICT state, the latter being highly stabilized in polar solvents. Since the first report of this interesting phenomenon by Lippert et al. in 1961,[20] several models have been proposed to elucidate the occurrence of dual fluorescence and to characterize the ICT state of DMABN and other structurally related molecules. According to the twisted intramolecular charge transfer (TICT) model, the dimethylamino and the benzonitrile groups of DMABN adopt a mutually perpendicular configuration in the charge transfer state, which leads to complete electronic decoupling between the two groups.[1,2] An alternative planar intramolecular charge transfer (PICT) model proposes that the dimethylamino and benzonitrile moieties have a predominantly coplanar structure.[3,21] The wagged intramolecular charge transfer (WICT) model suggests a rehybridization of the amino nitrogen from a planar sp^2 to a pyramidal sp^3 structure,[22] while the rehybridized intramolecular charge transfer (RICT) model suggests a rehybridization of the cyano carbon atom from sp to sp^2 involving a bent cyano bond.[23]

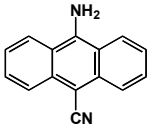

Scheme 1 Chemical structure of 9-amino-10-cyanoanthracene (ACAN).

Unlike DMABN, the analogous molecule without the N-methyl groups, i.e., 4-(amino)benzonitrile, shows only a single emission band from the LE state, irrespective of the polarity of the solvent medium.[24-26] The absence of dual emission in this molecule has been explained in terms of the large energy gap between the LE state and the higher lying ICT state, which prevents the population of the ICT state.[24,27] Similarly, the analogous naphthalene derivative, 1-amino-4-cyanonaphthalene, also shows a single emission band in a broad spectrum of solvent polarities.[28] Surprisingly, the presently studied anthracene derivative, 9-amino-10-cyanoanthracene (ACAN, Scheme 1), behaves in a completely different manner.[29-31] In addition to exhibiting two emission bands, this molecule also shows two distinct absorption bands corresponding to each of the two emissions. These features are observed in solvents of different polarities. This is in contrast to DMABN that shows a single

absorption band corresponding to its initial excitation to the LE state, although emission can occur from both LE and ICT states. It may be restated at this point that according to the TICT model, the ICT state which is responsible for the dual emission in DMABN, is reached by conformational change in the excited state in polar solvents, and cannot be attained by direct excitation. In this context, the dual absorption and emission behavior of ACAN appears to be quite intriguing and unusual compared to other known dual emission chromophores.

Following the observation of dual absorption and emission bands in ACAN, other structurally related molecules were found to display similar interesting behavior.[29-33] Although different theories have been proposed to rationalize the unusual behavior of these molecules, their photophysics is not yet completely understood. In the present study, we have examined the atypical photophysical properties of ACAN in polar and nonpolar solvents, and attempted to critically analyze the origin of its dual absorption and emission bands. We have undertaken rigorous purification methods to ensure the absence of any spurious absorption/emission from impurities. Isotope exchange studies as well as systematic temperature-dependent fluorescence measurements have been performed for the first time, to substantiate the observed results. The prototropic behavior of ACAN and the consequent effect on its dual absorption/emission behavior has also been investigated in detail.

Experimental section

The compound, 9-amino-10-cyanoanthracene (ACAN) was synthesized according to the procedure reported previously.[31,34] The sample was purified by recrystallization followed by HPLC (for details see Fig. S1, Note S1, ESI†). The solvents used in the present study were of spectroscopic grade and obtained from Spectrochem (India). No background absorption or emission was observed from the commercially obtained solvents; hence they were used without further purification. The solutions were freshly prepared prior to the experiments to avoid any possible degradation of the samples. The concentration of ACAN was maintained in the range of 3-15 μM (ε_{450nm}=10,230 M^{-1} cm^{-1}).[31] For studies under highly acidic conditions, the stability of ACAN was ascertained through ^{13}C NMR experiments (Fig. S2, Note S2, ESI†).

Absorption spectra were recorded with a Jasco UV-vis spectrophotometer (model V-650). Steady-state fluorescence spectra were measured with a Hitachi spectrofluorimeter (F-4510), maintaining a scan speed of 240 nm/min and excitation/emission slits of 5 nm. The fluorescence quantum yields (Φ_f) were estimated by a comparative method, using Coumarin-153 in ethanol solution as the reference (Φ_f=0.26).[35,36] Time-resolved fluorescence measurements were carried out using a time-correlated single photon counting (TCSPC) spectrometer (Horiba Jobin Yvon, UK). The samples were excited by light pulses from a diode laser source (375 nm or 445 nm, repetition rate of 1 MHz) and the fluorescence was detected using a PMT based detection module (model TBX4). The typical instrument response function (IRF) for the present setup is ~250 ps at the full-width at half-maximum. All measurements were carried out at the magic angle configuration to eliminate the contribution of the rotational depolarization of the dye on the observed fluorescence decays. The fluorescence decays were analyzed by reconvolution method, considering either mono-exponential or multi-exponential decay functions. The quality of the fits and consequently the mono-/multi-exponential natures of the decays were judged by the reduced chi-square (χ^2) values and the distribution of the weighted residuals among the data channels. For a good fit, the χ^2 value was close to unity and the weighted residuals were distributed randomly among the data channels.[35] The temperature of the experimental solution was controlled with a thermoelectric controller (TC 125, Quantum Northwest) within ±1°C.

Results and Discussion

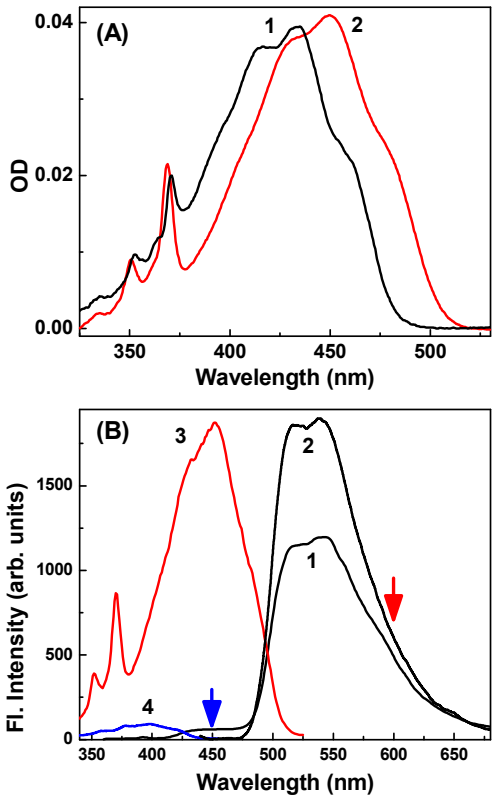

Fig. 1 (A) Absorption spectra of ACAN in (1) cyclohexane and (2) acetonitrile solutions. (B) Emission spectra of ACAN in acetonitrile on excitation at (1) 350 nm and (2) 435 nm and the corresponding excitation spectra for emission monitored at (3) 600 nm and (4) 450 nm (These wavelengths are also indicated with arrows).

Fig. 1A shows the absorption spectra of ACAN in cyclohexane (CH) and acetonitrile (ACN) solutions. In both the cases, a broad long wavelength absorption band (with maximum optical density, OD, around 430 nm in CH and around 450 nm in ACN) is accompanied by overlapping anthracene-like structured absorption bands in the region of ~350-390 nm. While the position of the shorter wavelength anthracene-like absorption bands remains unaffected by changing the solvent polarity, the longer wavelength absorption band shows a considerable redshift with increasing solvent polarity. For the convenience of discussion, henceforth we refer to the short wavelength absorption bands as AI and the longer wavelength bands as AII. The redshift in AII, with increasing solvent polarity, indicates

that this band arises due to transition to an excited state that is significantly more polar than the ground state. Previous studies have assigned this excited state as the ICT state of ACAN, involving charge transfer from the amino substituent to the cyano group.[29-31]

Fig. 1B shows the excitation and emission spectra of ACAN in acetonitrile solution. The emission spectra have been obtained with two different excitation wavelengths. When excited at 350 nm (a blue shifted wavelength chosen to selectively excite the absorption band, AI, with minimum overlap from AII band), two emission bands are observed; a weaker emission band in the blue region (~ 430-450 nm, henceforth referred as EI) and an intense emission band at the longer wavelength region with maximum around 547 nm (henceforth referred as EII). On excitation at 435 nm (chosen to selectively excite the longer wavelength absorption band, AII), only the EII emission band is observed with maximum around 547 nm. Similar behavior is also observed in the emission spectra of ACAN in the nonpolar solvent, cyclohexane (Fig. S3, ESI†).

To understand the origin of the dual emission of ACAN, excitation spectra were recorded for each of the two emission bands, EI and EII. When monitored at 450 nm (selective for emission EI), the excitation spectrum shows only the bands corresponding to the absorption, AI. However, when emission is monitored within the envelope of EII emission, at 600 nm (or even beyond 600 nm to selectively monitor EII avoiding any overlap with the EI emission), the excitation spectrum matches quite well with the entire absorption spectrum of ACAN. Thus, in this case, two excitation bands are clearly observed; one broad longer wavelength band with maximum around 450 nm, which corresponds to the absorption band AII and the other shorter wavelength anthracene-like structured excitation in the region of 350-390 nm that corresponds to the absorption band, AI. The appearance of both AI and AII like bands in the excitation spectra when monitored at 600 nm and beyond, suggests that the EII emission of ACAN originates from the excitation of the same molecule that is also responsible for the EI emission. Further support for this proposition is obtained from fluorescence lifetime measurements, as discussed below.

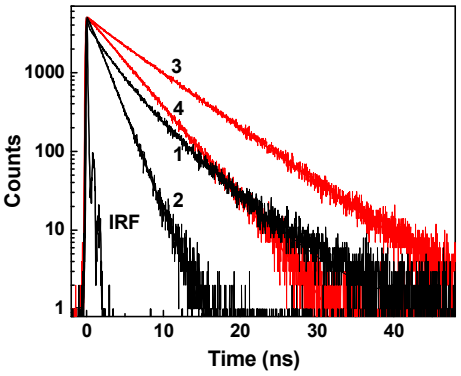

Fig. 2 Fluorescence decay traces of ACAN in cyclohexane (black) monitored at (1) 435 nm, (2) 550 nm and in acetonitrile (red) monitored at (3) 435 nm, (4) 550 nm. The excitation wavelength was 375 nm; IRF is the instrument response function

Fig. 2 shows the fluorescence decay traces for ACAN (excitation wavelength 375 nm) in ACN and CH solutions recorded at 435 and 550 nm, corresponding to the emission bands EI and EII, respectively. In both solvents, the decay traces at the two emission bands are distinctly different. The decay traces measured at 550 nm for EII can be fitted satisfactorily to a single exponential function with fluorescence lifetimes of 3.8 ns in ACN and 1.7 ns in CH. The single exponential nature of the decays is a clear indication that the EII emission band originates from a single emitting species with no overlapping contribution from any other fluorescent moiety. This observation thus corroborates well with the earlier presumption that the AI like band in the excitation spectrum, when emission is monitored in the EII band (e.g. at 600 nm, Fig. 1B) is not due to any fluorescent impurity but actually arises from the same molecule that also shows the AII band in the excitation spectrum.

Interestingly, unlike the EII emission, the decay traces of ACAN recorded at 435 nm (EI emission band) cannot be fitted satisfactorily to a single exponential function. In this case the decay traces are bi-exponential in nature, with fluorescence lifetime components of 6.3 ns (98%) and 0.8 ns (2%) in ACN solution and 4.8 ns (57%) and 2.2 ns (43%) in CH solution. It is evident that the biexponential nature of the decays for EI emission is not due to the overlapping EII emission, because none of the two lifetime components correspond to the lifetime value obtained for the EII emission. Intuitively, we feel that the short lifetime component (0.8 ns in ACN and 2.2 ns in CH) observed for the EI band could be due to some aggregation of ACAN in solution, while the longer lifetime component (6.3 ns in ACN and 4.8 ns in CH) possibly corresponds to the monomeric ACAN with anthracene-like chromophoric structure.[37,38] Since ACAN is very weakly soluble in the nonpolar solvent CH, the tendency of aggregation would be much higher in this solvent than in ACN. Accordingly, the contribution of the shorter lifetime component is expected to be higher in CH compared to ACN, which is in agreement with the observed results. The poor solubility of ACAN in CH precluded us from carrying out systematic concentration dependent studies. As an alternative approach, the fluorescence decay traces of ACAN were examined in different solvent mixtures of cyclohexane (CH) and ethylacetate (EA), with the idea that increasing the composition of the polar co-solvent EA, in the solvent mixture would prevent the aggregation of ACAN in solution. In this study we used EA instead of ACN as a polar co-solvent because ACN is not completely miscible with CH. The observed results in CH-EA mixtures indicate that the biexponential nature of the decays becomes gradually less pronounced as the percentage of EA is increased in the solvent mixture (Fig. S4, Table S1, ESI†). This observation supports our proposition that there is some aggregation of ACAN in the solution, and suggests that aggregation is considerably favoured in the nonpolar solvent, CH. The absorption and emission spectra of ACAN in CH-EA mixtures are presented in Fig. S5, ESI†.

At this juncture, and in the light of previous studies, it is possible to surmise the following: excitation of ACAN at longer wavelengths (AII band) directly populates the ICT state, which is the lowest excited singlet state, and leads to emission at longer wavelengths (EII emission, $S_1 \rightarrow S_0$). Excitation with shorter wavelength light (AI band), however, leads to the effective creation of two kinds of excited state populations; one of them at a relatively nonpolar, higher excited state that emits at shorter

wavelengths (EI emission) and another in a significantly polar lower ICT state, that emits at longer wavelengths (EII emission). The shorter wavelength absorption and emission bands resemble the $\pi\rightarrow\pi^*$ transitions of the unsubstituted parent molecule, anthracene. Since the EI emission appears at somewhat higher energies compared to the lowest energy absorption of ACAN (AII band), it can be justifiably assigned to the $S_2\rightarrow S_0$ fluorescence. Emission from excited states higher than S_1 is a rather unusual phenomenon and is in violation of Kasha's rule, which states that despite excitation to higher singlet states, emission always occurs from the lowest energy excited state, S_1, due to fast radiationless deactivation of the higher excited states to the lowest excited singlet state.[35,39] One of the notable exceptions to this rule is azulene, which shows predominant emission from the S_2 state. This happens due to the large energy gap between the S_2 and S_1 states of azulene that prevents the radiationless deactivation of the S_2 state.[35,39] Fluorescence from higher excited states is also reported for some other chromophores like aromatic acenes, polyenes, thioketones and metalloporphyrins.[40-42] In the case of ACAN, it has been proposed that the S_2 emission arises because of the poor electronic coupling between the S_2 and S_1 states (due to large conformational differences as discussed below), which reduces the radiationless deactivation of S_2 to the S_1 state.[31] Our present observation that the fluorescence decays of the two emission bands, EI and EII, are not correlated, also suggests that the S_2 and S_1 states of ACAN are not coupled with each other. Thus, the ICT (S_1) state of ACAN is not populated through the usual internal conversion process from the thermally equilibrated lowest vibrational level of the S_2 state. It is possible, however, that during excitation with light of shorter wavelengths, a small fraction of the molecules can populate the ICT state from the higher vibrational levels of the S_2 state. This fraction of the excited molecules that cross over to the ICT state is responsible for the EII emission. Since the S_2 and S_1 states are not strongly coupled, the majority of the excited molecules in the hot S_2 state undergo vibrational relaxation to the thermally equilibrated lowest vibrational level of S_2. These latter excited molecules are responsible for the EI emission. This process is depicted schematically in a potential energy diagram (discussed later). Such an excited state process can explain the appearance of both AI and AII like bands in the excitation spectra when monitored within the envelope of the EII emission (Fig. 1B). However, a direct proof for the above proposition could not be obtained from excitation wavelength dependent changes in the emission spectral characteristics of ACAN, possibly because of the large overlap between the AI and AII absorption bands.

Previous geometry optimization studies have shown that ACAN does not have a planar structure in the ground state. The amino group is twisted with respect to the plane of the aromatic ring with a torsion angle of about 21°.[31] This geometry is adopted by the molecule to avoid steric repulsion from the *peri*-hydrogens of the anthracene ring. Considering that the excitation of ACAN to the S_2 state resembles the $\pi\rightarrow\pi^*$ transitions of the unsubstituted parent molecule, anthracene, it can be inferred that the amino group of ACAN is not directly coupled to this electronic transition. It is quite likely therefore, that the twist angle of the amino group might not change to any significant extent in the S_2 state. This implies that ACAN retains its nonplanar ground state structure in the higher energy S_2 state. On the other hand, the S_1 state arises due to intramolecular charge transfer from the electron donating amino group to the electron withdrawing cyano group of ACAN. Due to the participation of the amino group in the ICT process, the geometry of ACAN in this excited state is expected to be quite different from the ground state and the S_2 state. The ICT state is likely to favor a more planar structure for ACAN, so as to facilitate the charge delocalization. This change in molecular geometry between the S_2 and S_1 states is proposed to be the basis for a poor electronic coupling between the two states and hence very weak S_2 to S_1 nonradiative transition in ACAN. Based on this model, it can be anticipated that the local motions of the amino group will not have much effect on the excited state dynamics of the S_2 state but will significantly influence the ICT character and hence the dynamics of the S_1 state. With this presumption, we examined the fluorescence decay dynamics for both EI and EII emission bands in H_2O and D_2O solutions, to understand the role of the amino group motions on the emission lifetimes of ACAN. The exchange of the hydrogen atoms in the amino group of ACAN with deuterium (conversion from $-NH_2$ to $-ND_2$ in the presence of D_2O) is indicated by the ^1H NMR spectra of ACAN (Note S3, Fig. S6, ESI†).

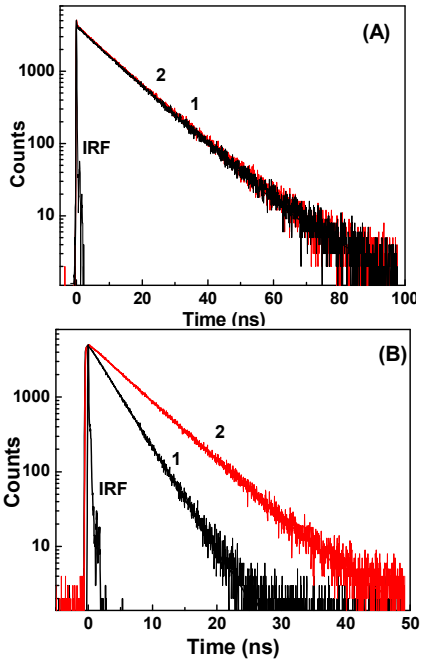

Fig. 3 (A) Fluorescence decay traces of ACAN at 435 nm, excitation wavelength = 375 nm; (1) H_2O (black) and (2) D_2O (red). (B) Fluorescence decay traces of ACAN at 550 nm, excitation wavelength = 445 nm; (1) H_2O (black) and (2) D_2O (red); IRF is the instrument response function.

In both H_2O and D_2O media, the decay traces for the EI emission (at 435 nm) are identical, with a fluorescence lifetime of 10.7 ns (Fig. 3A). This suggests that for the EI emission, the amino group of ACAN has no coupling with the electronic transition. A pronounced difference is, however, observed in the decay traces for the EII emission (measured at 550 nm), in H_2O and D_2O solutions (Fig. 3B). The fluorescence lifetime for the EII

emission is found to increase from 3.3 ns in H_2O to 5.5 ns in D_2O. Such a large increase (~ 40%) in the fluorescence lifetime on changing the solvent from H_2O to D_2O clearly suggests that the local motions of the amino group of ACAN are directly coupled to the decay dynamics of the EII emission (S_1, ICT state). Thus, the observed changes in the decay kinetics for the EI and EII emission bands of ACAN in H_2O and D_2O are in support of our proposition that the dual emission of ACAN is a consequence of the different conformational structures and hence weak electronic coupling between the S_1 and S_2 excited states.

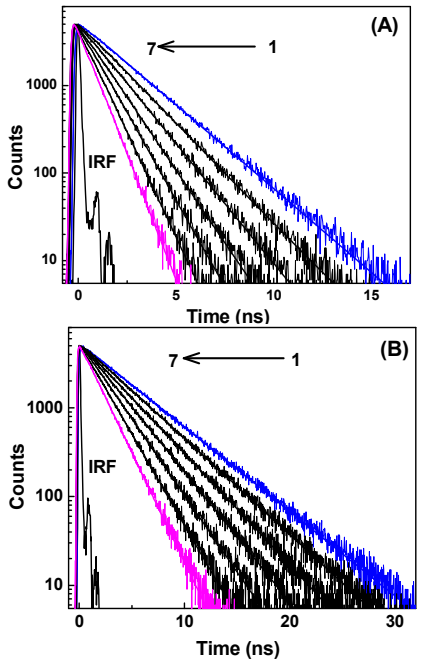

Fig. 4 Fluorescence decay traces of ACAN monitored at 550 nm in (A) cyclohexane and (B) acetonitrile at 10, 20, 30, 40, 50, 60 and 70°C (1-7). The excitation wavelength was 375 nm; IRF is the instrument response function.

Encouraged by the observed deuterium isotope effect, we investigated the effect of temperature on the fluorescence dynamics of the EII emission (550 nm) of ACAN in CH and ACN solvents. In both these media, the fluorescence decay traces show strong temperature dependence (Fig. 4), the fluorescence lifetimes, τ_f, becoming shorter with increasing temperature. The decay traces at all temperatures can be fitted to a single exponential function. Given that the radiative decay rate, k_f, is generally temperature independent for most fluorophores, the temperature effect on τ_f is expected to arise mainly through the nonradiative rate, k_{nr}.[35,43] For molecules in the excited state, the observed k_{nr} can have contributions from both activation-controlled and activationless nonradiative processes. For ACAN, since the τ_f values are strongly temperature dependent, we can assume that k_{nr} is mostly governed by the activation controlled nonradiative de-excitation channel.[4] Further, considering the fact that the amino group of ACAN is directly coupled to the decay dynamics of the EII emission; it is assumed that the major non-radiative de-excitation channel in this case is the internal conversion process determined by local motions of the amino group. The nonradiative de-excitation due to intersystem crossing, is indicated to be small (discussed later) and is not considered in the present analysis. Thus, the temperature dependent τ_f is expressed as a modified Arrhenius equation,[44]

$$\frac{1}{\tau_f} = k_f + k_{nr}^0 \exp\left(\frac{-\Delta E}{RT}\right) \quad (1)$$

where k_{nr}^0 is the pre-exponential factor and ΔE is the activation barrier for the nonradiative decay channel that is largely determined by the amino group motions. The radiative decay rate, k_f, can be calculated from the fluorescence quantum yield (Φ_f) using equation 2 and then used in equation 1 to correlate the temperature dependent τ_f values.

$$k_f = \frac{\Phi_f}{\tau_f} \quad (2)$$

For the present study, the quantum yields for the EII emission in both the solvents were determined at room temperature following a comparative method and using Coumarin-153 in ethanol solution as the reference (Φ_{ref}=0.26).[35,36] The samples were excited with 430 nm light for direct excitation to the ICT state of ACAN. The k_f value was subsequently obtained from equation 2 using the estimated Φ_f and τ_f values (Table 1). Fig.5 shows the plots for $1/\tau_f$ versus 1/T for ACAN in CH and ACN solvents. The k_{nr}^0 and ΔE values estimated by fitting these plots according to equation 1 are listed in Table 1.

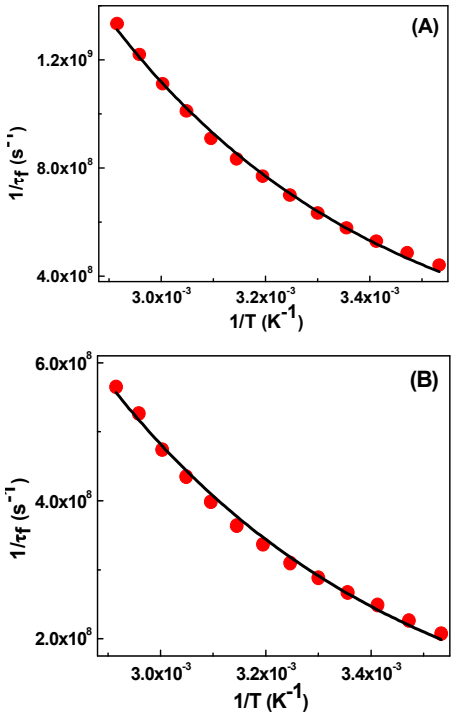

Fig. 5 Plots showing the temperature dependence of the fluorescence decay times of ACAN at 550 nm in (A) cyclohexane and (B) acetonitrile. The solid lines correspond to the fitted curves according to equation (1).

The ΔE value is found to be slightly higher in the nonpolar solvent, CH, than in the polar solvent, ACN. However, the k_{nr}^0 value is significantly higher in CH compared to ACN. This observation is consistent with earlier studies on amino substituted coumarin, anthraquinone and quinoline derivatives, where a "flip-

flop" motion of the amino group is proposed to play a major role in causing a fast nonradiative deactivation of the excited dyes in nonpolar solvents.[4,44-46] For the present case, an anti-twisting motion of the amino group coupled with the "flip-flop" movement of the amino hydrogens may be considered to be responsible for the nonradiative transition from the S_1 state to the ground state of ACAN.

Table 1 Photophysical parameters for the ICT emission of ACAN in cyclohexane and acetonitrile.

solvent	ε^a	λ_{em} (nm)	τ_f (ns)	φ_f	k_f (10^7) (s^{-1})	k_{nr}^0 (10^{11}) (s^{-1})	ΔE (kcal mol^{-1})
CH	2.02	524	1.7	0.03	1.7	3.3	4.6
ACN	36.6	548	3.8	0.07	1.7	0.9	3.5

[a] Dielectric constant.

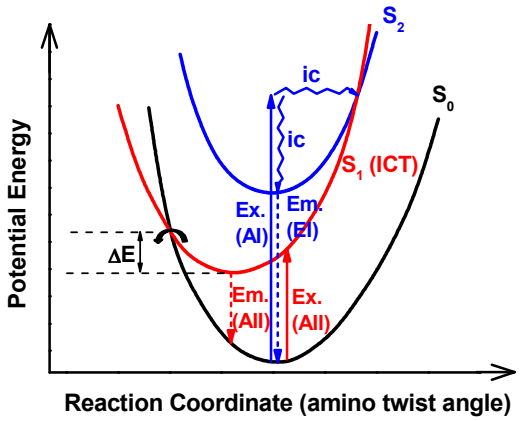

Fig.6 Schematic of the potential energy curves for ACAN.

Based on the present results and that reported in the literature,[4,28,44-46] the observed photophysical behavior of ACAN can be qualitatively understood from the conceptual potential energy (PE) diagram shown in Fig. 6, where the reaction coordinate would mainly be governed by the amino twist angle. In this diagram, the ground electronic state, S_0 and the higher excited singlet state, S_2, of ACAN are considered to have similar amino twist angles and correspond to nonplanar conformational structures. The twist angle of the amino group is expected to be very different in the first excited singlet state, S_1 (ICT state) of ACAN. Due to the direct involvement of the amino group in the charge transfer process, it is anticipated to adopt a more planar geometry with respect to the anthracene chromophore. In relation to the PE diagrams, such a large difference in the conformational structures would be realized as a relative displacement of the S_1 surface with respect to the S_0 surface and this would consequently lead to a crossing between the two PE surfaces. Accordingly, the excited ICT state of ACAN finds an activation-controlled nonradiative de-excitation channel to convert to the ground state through this crossing point. As Fig. 6 indicates, the activation energy, ΔE, for the de-excitation process, can be attained by the motions of the amino group and its interaction with the surrounding solvents. Such a proposition is supported by the observed deuterium isotope effect on the fluorescence decays of the EII emission of ACAN. The significant retardation in the motions of the amino group by the deuterium substitution of the amino hydrogens is reflected as the large increase in the fluorescence decay time of this emission in D_2O compared to H_2O. The appearance of both the emission bands, EI and EII, when excited with shorter wavelength light (AI band) is depicted in the above PE diagram in terms of the ICT (S_1) state being populated through the higher vibrational levels of the S_2 state. Qualitatively, a very steep crossing between the S_2 and S_1 states can be visualized that prevents significant coupling between these two energy states. As a result only a small fraction of molecules that cross over to the ICT state during the vibrational relaxation in the S_2 manifold gives rise to the EII emission, while the major fraction that relaxes in the potential well of the S_2 state gives rise to the EI emission.

Interestingly, although the isotope exchange has no effect on the dynamics of EI emission, the fluorescence decays at 435 nm (EI emission) are also found to be temperature dependent, to a reasonable extent (Fig. S7, ESI†). Clearly, the decrease in the fluorescence decay times of the EI emission with increasing temperatures cannot be attributed to activation controlled nonradiative de-excitation due to the amino group motions of ACAN. The other possible activation controlled nonradiative de-excitation process could be intersystem crossing.[47,48] To explore this possibility, the fluorescence decay traces of ACAN were recorded after purging the solutions with N_2 (Fig. S8, ESI†). A remarkable increase in the fluorescence decay time was observed for the EI emission (435 nm) of ACAN under N_2 purged conditions (6.8 ns to 9.9 ns, 45% increase). On the other hand, the increase in the fluorescence lifetime for the EII emission (550 nm) was comparatively smaller after purging with N_2 (3.8 ns to 4.2 ns, 10% increase). It is well known that fluorescence quenching by oxygen usually occurs due to intersystem crossing of the excited singlet to an excited triplet state.[35] Thus, the large increase in the fluorescence lifetime of the EI emission of ACAN upon removal of oxygen (by purging with N_2) clearly suggests that intersystem crossing is indeed a major de-excitation channel for the S_2 state. Based on the above results, we believe that the temperature dependence of the EI emission (S_2 state) arises primarily due to thermally activated intersystem crossing.

The interesting dual emission of ACAN even in the nonpolar solvent, CH, prompted us to explore its emission behavior in the solid state. Accordingly, emission spectra were recorded from a thin film of ACAN deposited on a quartz slide, with excitation at both 350 nm and 435 nm. (Note S4, Fig. S9, ESI†). The overall spectral features are similar to that observed for ACAN in solution. This result indicates that crossing between the excited-state potential energy surfaces (Fig. 6) is the main cause of the dual emission behavior of ACAN, which is not dependent on the polarity of the medium.

Considering the role of the amino group in the ICT process, the protonation of this group is expected to largely modulate the photophysical properties of ACAN. Fig. 7 shows the absorption spectra of ACAN in ACN solution with increasing concentration of H_2SO_4. It is observed that with increasing acid concentration, there is an increase in the absorption of the protonated form of ACAN (~340-415 nm) with a concomitant decrease in the AII absorption. At this point it is useful to recall that the AII band arises due to the direct excitation of ACAN to the ICT state. The

decrease in AII absorption in the presence of H_2SO_4 is therefore expected because protonation will diminish the electron donating ability of the amino group and hence prohibit the intramolecular charge transfer process. With increasing H_2SO_4 concentration, a clear isosbestic point is observed at 407 nm, in accordance with the two-state equilibrium between the protonated ($ACANH^+$) and neutral forms of ACAN, the latter showing the ICT absorption band, AII. The observation that the ICT absorption persists even upto a very high acid concentration suggests that the acidity constant, pK_a, of $ACANH^+$ is exceedingly low.

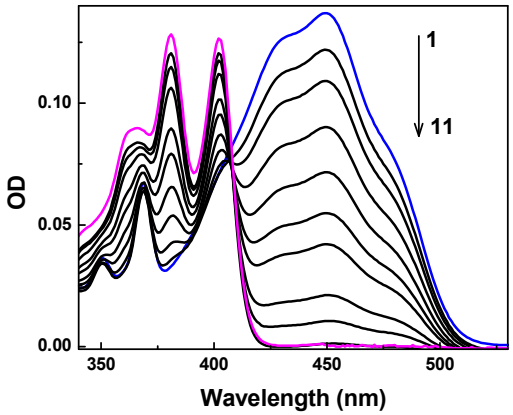

Fig. 7 Absorption spectra of ACAN in acetonitrile with different concentrations of H_2SO_4 (in mM): 0, 9, 18, 37, 56, 74, 92, 138, 184, 276, 460 (1-11).

To determine the pK_a value of $ACANH^+$ we carried out the acid titration studies in aqueous medium (5% methanol in water). Since the acid concentrations in the present cases are very high, we used the Hammett acidity function, H_0, instead of the pH scale.[49,50] The changes in the spectral characteristics of ACAN at different acid concentrations and the corresponding plot for the absorbance versus the H_0 values of the solution are shown in Fig. 8. The pK_a of $ACANH^+$ in water is thus estimated to be about -0.9 (Note S5, ESI†). The low pK_a value of $ACANH^+$ is understandable by comparison with a related anthracene derivative, 9-aminoanthracene, for which the pK_a of the conjugate acid form is reported to be about 2.7.[51] It is evident that the presence of the electron withdrawing cyano group at the 10-position of ACAN is responsible for the further reduction in the pK_a value of its conjugate acid form compared to the parent 9-aminoanthracene molecule.

Fig. 9A shows the emission spectra of ACAN at different acid concentrations. Although with increasing acid concentration the emission from the protonated form of ACAN (~400-470 nm, which overlaps with the EI emission of ACAN) continuously increases at the expense of the EII emission band from the ICT state (Inset Fig. 9A), the latter emission interestingly, persists even at a very high acid concentration. Thus, the emission from the ICT state (EII emission band) can be observed distinctly even at a H_2SO_4 concentration of 460 mM, where the corresponding absorption band (AII) effectively disappears in the absorption spectrum of ACAN (Fig. 7, trace number 11). This effect is also clearly demonstrated in the excitation spectra of ACAN, in the presence and absence of acid (Fig. 9B). When monitored at 600 nm (ICT emission band, EII) in the presence of high acid concentration (460 mM), the excitation spectrum shows only the bands corresponding to the absorption of the protonated form of ACAN. This implies that the EII emission under very high acid concentration evolves from the initially excited protonated form of ACAN. Therefore, the observation of dual emission in this particular situation of high acid concentration must be related to the excited state prototropic behavior of ACAN.

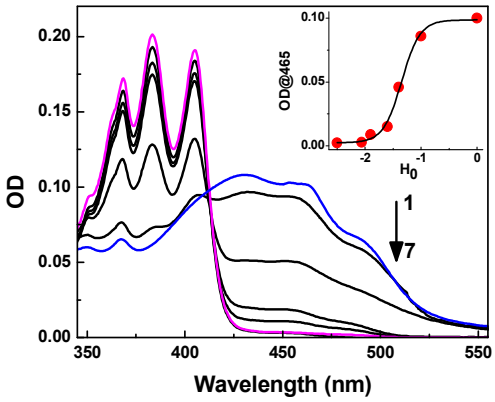

Fig. 8 Absorption spectra of ACAN in aqueous medium (5% methanol in water) with different H_2SO_4 concentrations (in M): 0, 2, 3, 3.5, 4, 4.5 and 5 (1-7). Inset show the plot of the absorbance at 465 nm versus the Hammett acidity function, H_0.

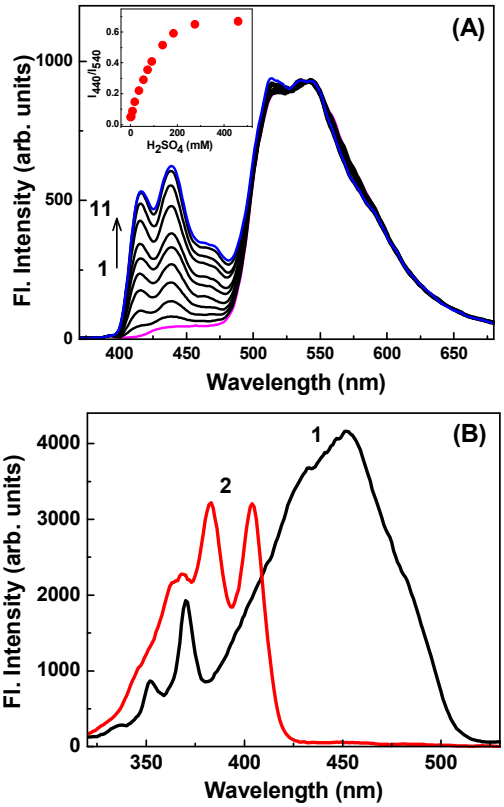

Fig. 9 (A) Emission spectra of ACAN in acetonitrile with varying concentrations of H_2SO_4 (in mM): 0, 9, 18, 37, 56, 74, 92, 138, 184, 276, 460 (1-11). Emission spectra have been corrected for the absorption changes at the excitation wavelength (350 nm) and the corrected spectra are presented after normalization with respect to the EII emission maximum. Inset shows the variation in the ratio of the emission intensities at 440 nm and 540 nm, with increasing acid concentration. (B) Excitation spectra of ACAN monitored for 600 nm emission in the (1) absence and (2) presence of 460 mM H_2SO_4.

The aminoanthracenes are known to have considerably higher acidities in the excited state compared to the ground state (e.g. pK_a* for the conjugate acid of 9-aminoanthracene is -6.1 compared to the ground state pK_a value of 2.7).[51] For $ACANH^+$, the excited state acidity constant pK_a* has been estimated to be about -9.3 using Förster's cycle method (Note S5, ESI†). Thus, when the H_0 value of the solution is lower than the ground state pK_a but higher than the excited state pK_a* of $ACANH^+$, dual fluorescence can easily be observed from both $ACANH^+$* and ACAN*, as the two species would be connected by an excited state prototropic process. For the present system, it is thus inferred that a part of the initially excited protonated form, $ACANH^+$* undergoes deprotonation to ACAN* even at a very high acid concentration, which in turn gives the characteristic emissions (EI and EII) and returns to the ground state before undergoing re-protonation.

Observation of fluorescence emission from both the protonated and neutral forms would certainly depend on the fluorescence lifetime of $ACANH^+$* and the deprotonation rate for its conversion to ACAN*. These aspects can be better understood from time-resolved fluorescence studies. The fluorescence decay traces of ACAN monitored at 435 nm and 550 nm in the absence and presence of varying H_2SO_4 concentrations are shown in Fig. 10. The kinetic data obtained by reconvolution analysis of these decays using suitable exponential functions, are presented in Table 2.

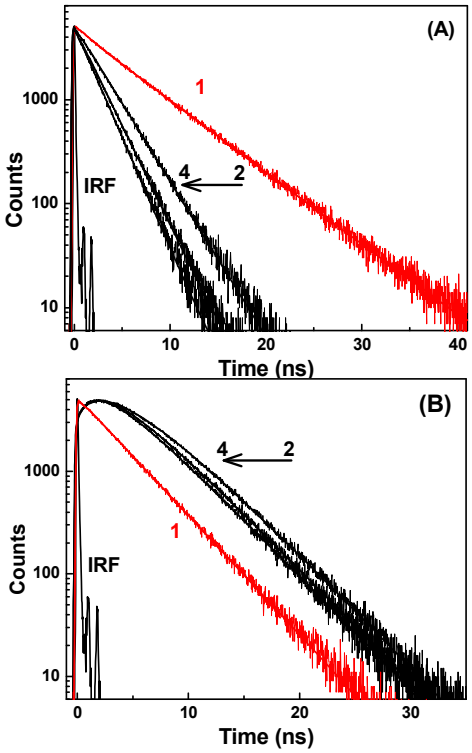

Fig. 10 Fluorescence decay traces of ACAN in acetonitrile for different concentrations of H_2SO_4 (in mM): 0 (1, red), 92, 276, 460 (black, 2-4); (A) monitoring wavelength = 435 nm and (B) monitoring wavelength = 550 nm. The excitation wavelength was 375 nm; IRF is the instrument response function.

On addition of acid, there is a considerable increase in the fluorescence decay rate of ACAN at 435 nm. The observed decay times of ~2.8-2.0 ns, in the presence of acid, is attributed to the protonated form, $ACANH^+$*. It is proposed that this decay time is due to the combined effect of the natural fluorescence decay of $ACANH^+$* and the deprotonation rate of $ACANH^+$* to form ACAN*. The generated ACAN* is expected to decay with a lifetime of 6.3 ns corresponding to the EI emission from the neutral form of ACAN as observed in neutral aqueous solution. However, the strong overlapping emission of $ACANH^+$* effectively masks the weak EI emission at 435 nm, and as a result no long lifetime component corresponding to ACAN*could be detected in the decay traces monitored at this wavelength in the presence of acid (Table 2). The slight reduction in the fluorescence decay time of $ACANH^+$* (2.8 ns to 2.0 ns; Table 2) with increasing acid concentration is possibly due to the change in the solvent environment as the acid concentration is gradually increased to a large extent. Corresponding with the decay time of ~2.8-2.0 ns for the protonated form at 435 nm, a growth component is distinctly observed in the fluorescence traces monitored at 550 nm. This growth component clearly indicates the formation of the ICT state of ACAN* from the initially excited protonated form of the molecule, $ACANH^+$*. The generated ACAN* subsequently decays to the ground state with the characteristic fluorescence decay time of ~ 3.8 ns for the ICT emission (EII emission, 550 nm). The tunability of the absorption and emission spectral characteristics of ACAN under strongly acidic conditions is a very interesting observation for the present molecule. This property is likely to have implications in the design and development of molecular probes that exhibit desired protonation dependent optical response for sensing applications or molecular logic gate functions. Overall, the present studies on ACAN under various conditions of solvent polarity, deuterium isotope effect, temperature dependence and solution acidity provide a detailed understanding on the interesting photophysical properties and dual absorption/emission behavior of this molecule.

Table 2 Fluorescence decay parameters (lifetimes and amplitudes)[a] of ACAN in acetonitrile at 435 nm and 550 nm in the presence of different concentrations of H_2SO_4. The excitation wavelength was 375 nm

H_2SO_4 (mM)	435 nm				550 nm			
	a_1	τ_1 (ns)	a_2	τ_2 (ns)	a_1	τ_1 (ns)	a_2	τ_2 (ns)
0	0.14	6.3	0.03	0.8	0.15	3.8	-	-
92	0.16	2.8	-	-	1.09	3.8	-1.00	2.8
276	0.16	2.2	-	-	0.51	3.8	-0.43	2.2
460	0.16	2.0	-	-	0.43	3.8	-0.35	2.0

[a] The fluorescence decays were fitted by considering either single or bi-exponential functions; $I(t) = \sum_i a_i \exp(-t/\tau_i)$

Conclusions

This study provides new insight into the unusual photophysical properties of 9-amino-10-cyanoanthracene (ACAN) that belongs to the important class of donor-acceptor substituted chromophores exhibiting intramolecular charge transfer (ICT) character. ACAN shows dual absorption and emission behavior, irrespective of the solvent polarity. The longer wavelength absorption and emission bands of ACAN (AII and EII) arise due to the direct transitions to and from the ICT state which is also

the first excited state (S_1) of the molecule. The shorter wavelength absorption and emission bands (AI and EI) are attributed to the transitions between the ground (S_0) and S_2 states. Thus, ACAN appears to be one of the few molecules that show emission from the higher excited state, S_2, in violation of Kasha's rule. The emission from the S_2 state of ACAN is attributed to arise mainly because of the weak electronic coupling between the S_2 and ICT (S_1) states of the molecule, due to the largely different conformational geometries in the two states. The different twist angles of the amino group of ACAN in the ICT state and the ground state results in a relative displacement and a consequent crossing of the PE surfaces of these two states. This eventually leads to the activation controlled nonradiative decay for the ICT state, assisted by the motions (flip-flop and anti-twisting) of the amino group in ACAN. The participation of the amino group motions in the de-excitation dynamics of the ICT state has been established by the deuterium isotope effect on the fluorescence lifetime of this state. The results have been explained with suitable mechanisms and qualitative PE diagrams. The present work also reveals the intriguing excited state prototropic behavior of ACAN in solution and highlights the acid induced tunability of its ICT emission at extremely high acid concentrations.

Notes and references

[a] *Radiation & Photochemistry Division, Bhabha Atomic Research Centre, Mumbai 400 085, India. E-mail: sharmidc@barc.gov.in*
[b] *Center for Biomedical Engineering and Technology, University of Maryland School of Medicine, 725 W. Lombard St., Baltimore, MD 21201, United States. E-mail: palakkadan@yahoo.com*

†Electronic Supplementary Information (ESI) available: [Purification and stability of the sample, exchange of amino hydrogens with deuterium, determination of pK_a and pK_a*, additional figures, Fig. S1-S9.]. See DOI: 10.1039/ b000000x/

1 Z. R. Grabowski, K. Rotkiewicz and W. Rettig, *Chem. Rev.*, 2003, **103**, 3899.
2 J. F. Letard, R. Lapouyade and W. Rettig, *J. Am. Chem. Soc.*, 1993, **115**, 2441.
3 T. Yoshihara, S. I. Druzhinin and K. A. Zachariasse, *J. Am. Chem. Soc.*, 2004, **126**, 8535.
4 S. Nad and H. Pal, *J. Phys. Chem. A*, 2001, **105**, 1097.
5 T. Soujanya, R. W. Fessenden and A. Samanta, *J. Phys. Chem.*, 1996, **100** 3507.
6 A. P. Kulkarni, Y. Zhu, A. Babel, P.-T. Wu and S. A. Jenekhe, *Chem. Mater.*, 2008, **20** 4212.
7 X. Peng, F. Song, E. Lu, Y. Wang, W. Zhou, J. Fan and Y. Gao, *J. Am. Chem. Soc.* , 2005, **127**, 4170.
8 W. Rettig, *Appl. Phys. B*, 1988, **45**, 145.
9 D. M. Shin, K. S. Schanze and D. G. Whitten, *J. Am. Chem. Soc.*, 1989, **111**, 8494.
10 J. N. Wilson and U. H. F. Bunz, *J. Am. Chem. Soc.* , 2005, **127**, 4124.
11 J. Bourson and B. Valeur, *J. Phys. Chem.*, 1989, **93** 3871.
12 G. S. Cox, P. J. Hauptman and N. J. Turro, *Photochem. Photobiol.*, 1984, **39**, 597.
13 R. Misra, R. Sharma and S. P. Bhattacharyya, *J. Comp. Methods in Sciences and Engineering* 2010, **10**, 149.
14 W. Rettig, *Angew. Chem., Int. Ed. Engl.* , 1986, **25**, 971.
15 J. Y. Lee, B. J. Minh, S. Mukamel and K. S. Kim, *J. Chem. Phys.*, 2003, **119**, 7519.
16 V. Mohan, A. Nijamudheen, S. K. Das, P. K. Sahu, U. P. Kar, . A. Rahaman and M. Sarkar, *Chem. Phys. Chem.,* 2012, **13**, 3882.
17 S. K. Das, A. S. Patra, D. Jose and M. Sarkar, *Chem. Phys. Lett.* 2012, **528**, 11.
18 J. Catálan, *Phys. Chem. Chem. Phys*., 2013, **15**, 8811.
19 K. Santhosh, A. Samanta, *Chem. Phys. Chem.*, 2012, **13**, 1956.
20 E. Lippert, W. Lüder, F. Moll, W. Nägele, H. Boos, H. Prigge and I. Seibold-Blankenstein, *Angew. Chem.* , 1961, **73**, 695.
21 Y. V. Il'ichev, W. Kühnle and K. A. Zachariasse, *J. Phys. Chem. A*, 1998, **102**, 5670.
22 W. Schuddeboom, S. A. Jonker, J. M. Warman, U. Leinhos, W. Kuehnle and K. A. Zachariasse, *J. Phys. Chem.*, 1992, **96**, 10809.
23 A. L. Sobolewski and W. Domcke, *Che. Phys. Lett.*, 1996, **250**, 428.
24 K. A. Zachariasse, T. vonderHaar, A. Hebecker, U. Leinhos and W. Kuhnle, *Pure & Appl. Chem.*, 1993, **65**, 1745.
25 S. Jiang and D. H. Levy, *J. Phys. Chem. A* 2002, **106**, 8590.
26 S. I. Druzhinin, A. Demeter, V. A. Galievsky, T. Yoshihara and K. A. Zachariasse, *J. Phys. Chem. A*, 2003, **107**, 8075.
27 I. Gómez, M. Reguero, M. Boggio-Pasqua and M. A. Robb, *J. Am. Chem. Soc.*, 2005, **127**, 7119.
28 K. Suzuki, A. Demeter, W. Kuhnle, E. Tauer, K. A. Zachariasse, S. Tobitab and H. Shizukab, *Phys. Chem. Chem. Phys.*, 2000, **2**, 981.
29 S. Muralidharan and K. Yates, *Chem. Phys. Lett.*, 1992, **192**, 571.
30 S. Muralidharan, H. K. Sinha and K. Yates, *J. Phys. Chem.*, 1991, **95**, 8517.
31 S. Muralidharan, A. J. Lough and K. Yates, *J. Photochem. Photobiol. A: Chem.*, 1993, **71**, 245.
32 S. Muralidharan and K. Yates, *J . Chem. Soc., Chem. Commun.*, 1991, 250.
33 S. Druzhinin, A. Demeter, M. Niebuer, E. Tauer and K. A. Zachariasse, *Res. Chem. Intermed.*, 1999, **25**, 531.
34 R. G. Landolt and H. R. Snyder, *J. Org. Chem.*, 1968, **33**, 403.
35 J. R. Lakowicz, *Principles of Fluorescence Spectroscopy*, 3rd ed., Springer, New York, **2006**.
36 M. K. Singh, H. Pal, A. C. Bhasikuttan and A. V. Sapre, *Photochem. Photobiol.*, 1998, **68**, 32.
37 R. Varghese and H-A. Wagenknecht, *Chem. Eur. J.*, 2010, **16**, 9040.
38 P. Verma and H. Pal, *J. Phys. Chem. A,* 2013, **117**, 12409.
39 M. Kasha, *Disc. Faraday Society*, 1950, **9**, 14.
40 D. W. Cho, M. Fujitsuka, J. H. Ryu, M. H. Lee, H. K. Kim, T. Majima and C. Im, *Chem. Commun.*, 2012, **48**, 3424.
41 B. Jana and N. Chattopadhyay, *J. Phys. Chem. A*, 2012, **116**, 7836.
42 T. Itoh, *Chem. Rev.*, 2012, **112**, 4541−4568.
431 K. K. Rohatgi Mukherjee, *Fundamentals of Photochemistry*, Wiley Eastern, New Delhi, **1978**.
44 H. Pal, S. Nad and M. Kumbhakar, *J. Chem. Phys.*, 2003, **119**, 443.
45 D. Panda and A. Datta, *J. Chem. Phys.*, 2006, **125**, 054513.
46 P. Dahiya, S. Dutta Choudhury, D. K. Maity, T. Mukherjee and H. Pal, *Spectrochim. Acta A*, 2008, **69**, 134.
47 N. J. Turro, *Modern Molecular Photochemistry*, University Science Books, California, **1991**.
48 R. G. Bennett, P. J. McCartin, *J. Chem. Phys.*, 1966, **44**, 1969.
49 T.N. Das, *Ind. Eng. Chem. Res.*, 2005**, 44***,* 1660.
50 T.N. Das, *Radiation Induced Free Radical Chemistry: In Homo & Heterogenous Media;* Dey, G. R. Ed.; Research Signpost: Trivandrum, 2008; pp 39-65.
51 K. Rotkiewicz and Z. R. Grabowski, *Trans. Faraday Soc*, 1969, **65**, 3263.